IEEE Access
Multidisciplinary | Rapid Review | Open Access Journal

SPECIAL SECTION ON KEY ENABLING TECHNOLOGIES FOR PROSUMER ENERGY MANAGEMENT

Received July 1, 2020, accepted July 15, 2020, date of publication July 23, 2020, date of current version August 5, 2020.

Digital Object Identifier 10.1109/ACCESS.2020.3011563

Energy Recovery Strategy Based on Ideal Braking Force Distribution for Regenerative Braking System of a Four-Wheel Drive Electric Vehicle

ZHENGWEI MA [1,2] AND DAXU SUN [3]

[1]College of Urban Transportation and Logistics, Shenzhen Technology University, Shenzhen 518118, China
[2]College of Mechatronics and Control Engineering, Shenzhen University, Shenzhen 518060, China
[3]Foshan Polytechnic, Foshan 528137, China

Corresponding author: Daxu Sun (sundx55@126.com)

This work was supported in part by the National Natural Science Foundation of Guangdong Province under Grant 2018A030310523; in part by the Special Innovation Project in Higher Education of Guangdong Province under Grant 2018KTSCX351; in part by the Ordinary University Engineering Technology Development Center Project of Guangdong Province under Grant 2019GCZX006; in part by the Science and Technology Development Foundation of Shenzhen Government under Grant JCYJ20190813111203628; and in part by the Teaching Reform Project in Higher Education of Guangdong Province (Title: Study on the Practical Teaching System of Multi-Integration of School-Enterprise and Industry-Education for Automotive Service Engineering Major Under the Background of New Engineering).

ABSTRACT Under raising pressure of global energy and environmental issues in recent years, electric vehicles (EVs) have been an alternative solution of the automobile industry owing to its high energy efficiency, low noise, and zero emission. However, the short driving range is an urgent problem to be solved for EVs. Energy recovery is an important technology to improve energy efficiency and extend driving range of EVs. In this paper, an improved braking energy recovery strategy based on ideal braking force distribution (curve I) was proposed for the regenerative braking system (RBS) of a small four-wheel drive (FWD) EV. Compared with previous study, the improved braking energy recovery strategy gives more consideration to braking stability and covers broader braking situations of the vehicle. The braking energy recovery strategy is extensively validated through numerical simulations of a previously built vehicle system model under different fixed braking strength and continuously varying braking strength. The simulation results show that the proposed braking energy recovery strategy is able to effectively achieve the regenerative braking function under different braking conditions while ensuring braking efficiency and braking stability.

INDEX TERMS Electric vehicle, energy recovery, braking stability, ideal braking force distribution.

I. INTRODUCTION

Due to the continuous depletion of global nonrenewable fossil fuels, the energy crisis is becoming more prominent than ever [1]. To mitigate the energy crisis, researchers have been making a lot of efforts in the fields of renewable energy [2]–[4], energy recovery [5]–[8], energy storage [9], [10], energy efficiency [11]–[14] *et al.* In automobile industry, electric vehicles (EVs) have been an alternative solution owing to its high energy efficiency, low noise, and zero emission [15]. However, the short driving range is an urgent problem to be solved. Regenerative braking plays an important role in improving energy efficiency and extending driving range of EVs, particularly in urban road conditions with frequent start-stop or acceleration-deceleration drive patterns. When EV is in braking, the regenerative braking system (RBS) can convert the kinetic energy or potential energy of the vehicle into electrical energy to charge the power battery, and provide motor braking torque to assist braking and reduce the brake temperature rise. Therefore, RBS not only realizes the recovery of regenerative braking energy, but also improves the braking efficiency and braking safety performance.

For most EVs, the hybrid braking system (HBS) is the most often form of braking system in which the friction braking and the electric motor braking are both used. In order to obtain better braking energy recovery capacity and maintain in braking safety, reasonable braking energy recovery strategy or hybrid braking force distribution strategy are essential.

The associate editor coordinating the review of this manuscript and approving it for publication was Jiayong Li.

There are a lot of research work focusing on the cooperative control strategy between the friction braking system and the RBS for both pure EVs and hybrid electric vehicles (HEVs) in the literature. In [16], the braking energy recovery of a RBS for HEV was validated through hardware-in-the-loop (HIL) simulation method. And then, a regenerative braking algorithm with continuously variable powertrain (CVT) ratio control was proposed in [17]. In [18], a regenerative braking energy management strategy for mild HEV was presented to maximize the braking energy recovery under the pre-condition of the Economic Commission for Europe (ECE) braking regulation (ECE R13). In [19] and [20], the cooperative control for regenerative braking and friction braking to increase energy recovery was studied, and a cooperative control algorithm was developed for automatic powertrain (AT) HEV. In [21], a series of simulations based on advanced regenerative braking strategies were conducted for plug-in HEV. In [13] and [22], a potential field approach-based trajectory control for autonomous EVs with in-wheel motors was studied, and a RBS configuration with new braking torque distribution strategy was proposed to improve energy recovery efficiency. In [23], two braking control methods were compared for a front wheel driven EV, and the energy recovery could be improved from 3.7% to 11.2%. In the case of normal braking, the braking force distribution between the front and rear wheels would affect the braking energy recovery efficiency. One popular distribution method was to make the braking force be proportional to the tire normal load [24]. In [25], the authors proposed a braking energy recovery strategy based on ideal braking force distribution (curve I), and analyzed its effectiveness under different braking strength through simulations.

The studies above are mainly carried out under the situations of decelerating and braking. During driving, the kinetic energy of the vehicle can be recovered under three situations which are respectively decelerating, braking, and coasting. Compared with the decelerating and braking situations, only a few researchers studied the regenerative braking under coasting situations [26]–[30], especially for pure EVs. In [26] and [27], the regenerative braking of a HEV in coasting mode was investigated, and a braking energy recovery strategy was proposed, which applied maximum motor braking torque to speeds above a certain threshold speed, and provided only friction brakes at low speeds. In [28], the adaptive-learning regeneration control for the EV in coasting mode was presented, but the control algorithm needs large amount of calculation and was not suitable for real time control. The authors in [29] studied the coasting control for EV based on the driving feeling. Simulation results demonstrated that the state of charge (SOC) of the battery could be increased by 0.036% and 0.021% in the initial speed of 100 km/h and 50 km/h, respectively. In [30], an energy recovery mode with the control strategy based on driver's intention was presented for RBS of EV, in which the energy recovery and driving range could be improved by 15.8% and 8.81% respectively compared with benchmark mode.

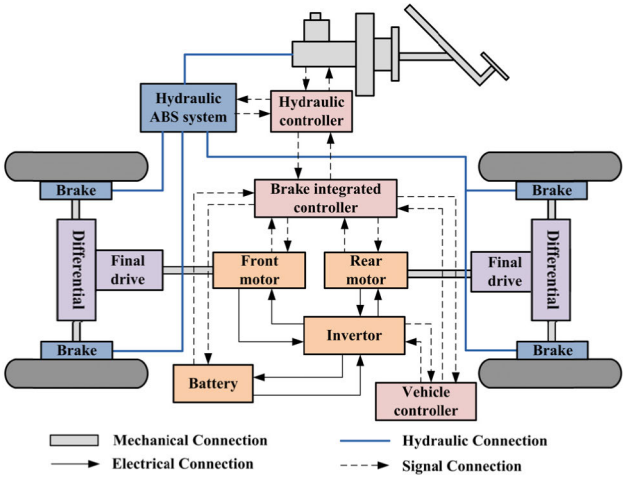

FIGURE 1. The RBS configuration of the FWD EV.

From the existing study, it can be found that there is a conflict between the braking energy recovery efficiency and the braking stability for the RBS of pure front-drive EV or pure rear-drive EV. The RBS of four-wheel drive (FWD) EV can obtain the maximum braking energy recovery capacity through reasonable braking force distribution between the front and rear axles on the premise of ensuring vehicle braking stability [14], [21], [22]. The main contribution of this paper is an improved braking energy recovery strategy based on the authors' previous study in [25]. Compared with previous study, the improved braking energy recovery strategy gives more consideration to braking stability and covers broader and more realistic braking situations of the vehicle. It is designed for the RBS of a small FWD EV.

The rest of the paper is organized as follows. In Section II, the vehicle system model is briefly introduced, including the RBS configuration, the vehicle subsystem models, and the parameters of the whole vehicle, motor and battery. Section III describes the improved braking energy recovery strategy based on ideal braking force distribution (curve I) of the FWD EV RBS. Simulations under different fixed braking strength and continuously varying braking strength, and analyses of the proposed energy recovery strategy are presented in Section IV. Finally, conclusions are given in Section V.

II. SYSTEM MODEL

In this paper, a small FWD EV with dual motors providing torque respectively for the front and rear axles is used as a platform to design the RBS and energy recovery strategy. The RBS configuration of the FWD EV is shown in Figure 1. It consists of two parts which are conventional friction braking subsystem and electrical motor braking subsystem, respectively. The RBS configuration can realize the free switch of pure front-drive, pure rear-drive and FWD of the EV according to different driving conditions and the driver's needs, so as to maximize the utilization of the adhesion coefficient of the front and rear wheels. In FWD mode,

TABLE 1. The whole vehicle parameters of the FWD EV.

Parameter	Value
Curb weight m (kg)	1250
Wheel base L (m)	2.40
Front track width l_f (m)	1.49
Rear track width l_r (m)	1.48
Distance from the center of gravity to front axle a (m)	1.20
Distance from the center of gravity to rear axle b (m)	1.20
Height of the center of gravity h_g (m)	0.54
Wheel rotational inertia J_w (kg·m^2)	0.6
Tire type number	175/70 R13
Sprung mass m_s (kg)	1167
Front unsprung mass m_{uf} (kg)	41.5
Rear unsprung mass m_{ur} (kg)	41.5
Final drive ratio i_0	5.46
Frontal area A (m^2)	2.2
Air resistance coefficient C_D	0.33

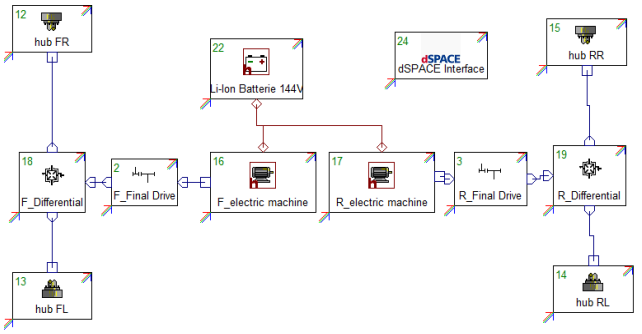

FIGURE 2. The vehicle transmission system model built in AVL CRUISE.

it can obtain better braking energy recovery capacity through reasonable braking force distribution between the front and rear axles while ensuring vehicle braking stability.

The vehicle system model of the FWD EV has been established in previous study which can be seen in authorised articles [25], [31], [32]. The subsystem models, including motor model and battery model, final drive model, differential model, hydraulic braking system model *et al.*, were built in AVL CRUISE environment by modular and parametric modeling method. Table 1 shows the whole vehicle parameters of the FWD EV. Figure 2 shows the transmission system model built in AVL CRUISE. The same motor is used for the front and rear axles of the FWD EV. The electrical motor and battery utilized in the model are respectively permanent magnetic brushless DC motor and lithium ion battery with the main parameters listing in Table 2 and Table 3.

The controller model is developed in MATLAB/Simulink which is shown in Section 3. In model simulation, the vehicle system model established in AVL CRUISE is embedded in MATLAB/Simulink by co-simulation interface in the form of S-Function.

TABLE 2. The main parameters of electrical motor.

Parameter	Value
Norminal voltage (V)	144
Rotational inertia (kg·m^2)	0.15
Weight (kg)	18
Rated speed (rpm)	2000
Maximum speed (rpm)	3750
Maximum electric current (A)	150
Maximum generating current (A)	150
Maximum working temperature (°C)	170
Peak power (kW)	20
Rated power (kW)	10

TABLE 3. The main parameters of lithium ion cell.

Parameter	Value
Nominal capacity (Ah)	10
Norminal voltage (V)	3.2
Maximum voltage (V)	4.2
Minimum voltage (V)	2.2
Average charging internal resistance (mΩ)	0.8
Average discharge internal resistance (mΩ)	0.6

III. BRAKING ENERGY RECOVERY STRATERGY

A. IDEAL BRAKING FORCE DISTRIBUTION

When the vehicle is in braking, the condition that front wheel and rear wheel are locked simultaneously is most beneficial to both the full use of the attachment conditions and the vehicle direction stability. It is an ideal case, in which front wheel and rear wheel are in ideal braking force distribution, and is named to curve I.

The situation that front wheel and rear wheel are in ideal braking force distribution (curve I) is as follows:

$$\begin{cases} F_{\mu 1} + F_{\mu 2} = \varphi G \\ F_{\mu 1} = \varphi F_{Z1} \\ F_{\mu 2} = \varphi F_{Z2} \end{cases} \tag{1}$$

Or

$$\begin{cases} F_{\mu 1} + F_{\mu 2} = \varphi G \\ \dfrac{F_{\mu 1}}{F_{\mu 2}} = \dfrac{F_{Z1}}{F_{Z2}} \end{cases} \tag{2}$$

where $F_{\mu 1}$ and $F_{\mu 2}$ are respectively the braking force of front wheel and rear wheel. F_{Z1} and F_{Z2} are respectively the ground normal reaction force of front wheel and rear wheel. G is the gravity of the vehicle. φ is the adhesion coefficient of tire-road.

In order to analysis the braking force distribution of front wheel and rear wheel under different braking conditions,

the braking strength z can be given as:

$$z = \frac{\dot{v}_d}{g} \tag{3}$$

where $\dot{v}_d$ is the braking deceleration. g is the acceleration of gravity, $g = 9.8m/s^2$.

When the vehicle is in braking, the ground normal reaction force of front wheel and rear wheel is as follows:

$$\begin{cases} F_{Z1} = \dfrac{G\left(b + zh_g\right)}{L} \\ F_{Z2} = \dfrac{G\left(a - zh_g\right)}{L} \end{cases} \tag{4}$$

where a and b are respectively the longitudinal distance from the center of gravity (CG) to front axle and rear axle. L is the wheel base, thus, $L = a + b$. h_g is the height of vehicle CG.

When front wheel and rear wheel are in ideal braking force distribution (curve I), $z = \varphi$. Submitting (4) to (2), (2) can be expressed as:

$$\begin{cases} F_{\mu 1} + F_{\mu 2} = \varphi G \\ \dfrac{F_{\mu 1}}{F_{\mu 2}} = \dfrac{b + \varphi h_g}{a - \varphi h_g} \end{cases} \tag{5}$$

If the adhesion coefficient of tire-road φ is replaced by braking strength z, (5) can be rewritten as:

$$\begin{cases} F_{\mu 1} + F_{\mu 2} = zG \\ \dfrac{F_{\mu 1}}{F_{\mu 2}} = \dfrac{b + zh_g}{a - zh_g} \end{cases} \tag{6}$$

In real application, if the braking force distribution of the front and rear wheels is above curve I, the rear wheels will be locked first and the vehicle is prone to side slip on the rear axle, which is a very dangerous and unstable braking condition. In order to ensure braking stability and maximize the use of adhesion conditions, the braking force distribution of the front and rear wheels must be below curve I and as close as possible to curve I.

B. CONTROL STRATERGY

In this study, the vehicle braking state is divided into two conditions, which are normal braking condition ($0 < z < 0.7$), and emergency braking condition ($z \geq 0.7$), respectively. The RBS in this study mainly works in normal braking condition. In case of normal braking ($0 < z < 0.7$), the main objective is to recover as much braking energy as possible while ensuring the braking efficiency and braking stability. For this purpose, the braking force distribution strategy between electric motor braking and hydraulic braking under different braking strength and adhesion coefficient of tire-road is proposed later.

In case of emergency braking ($z \geq 0.7$), the main objective is to make the vehicle wheel slip ratio track the optimal slip ratio to minimize the braking distance. Therefore, the braking energy recovery is not considered and the motor's regenerative braking function is turned off.

In addition, the motor's regenerative braking function will also be turned off when motor speed is lower than the lower limit (generally 500r/min), because the back electromotive force of the internal armature of the motor is too low to provide effective braking energy recovery.

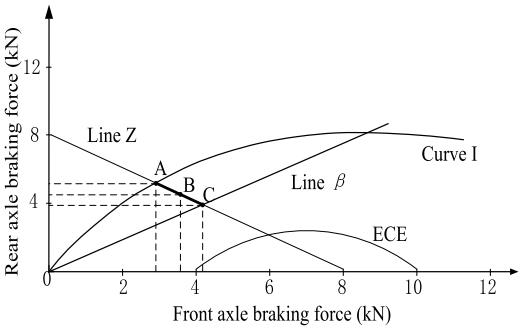

FIGURE 3. Braking force distribution strategy based on curve I.

In case of normal braking ($0 < z < 0.7$), the braking force distribution strategy is proposed as shown in Figure 3. The main idea is to ensure the braking force distribution of the front and rear axles meeting curve I. If the braking force distribution can not meet curve I, it should be below curve I and meet the total braking force requirements and ECE regulations. In Figure 3, line Z is the total braking force requirement of the front and rear axles. Line β is the hydraulic braking force distribution of the front and rear axles. Point A is the intersection of curve I and line Z, which meets both the total braking force requirement and the ideal braking force distribution. Point C is the intersection of line B and line Z, which meet both the total braking force requirement and the hydraulic braking force distribution. Point B is a point on line Z and between point A and point C, on which the vehicle's braking efficiency and braking stability are better than that of pure hydraulic braking, but weaker than that of the ideal braking force distribution. The braking force distribution strategy is proposed as follows.

The compound braking force of the front and rear axles from electric motor braking and hydraulic braking should first be distributed as point A. If it can not meet point A, the electro-hydraulic compound braking force should be distributed as point B. When the motor's regenerative braking function is turned off, the braking force is distributed as point C.

The braking force of the front and rear axles is composed of hydraulic braking force and electric motor braking force, which can be expressed as:

$$\begin{cases} F_{xb1} = F_{hy\_F} + F_{reg1} \\ F_{xb2} = F_{hy\_R} + F_{reg2} \end{cases} \tag{7}$$

where F_{xb1} and F_{xb2} are respectively the total braking force of front axle and rear axle. F_{hy_F} and F_{hy_R} are respectively the hydraulic braking force of front axle and rear axle. F_{reg1} and F_{reg2} are respectively the electric motor braking force of front axle and rear axle.

In order to ensure braking stability, the braking force of front axle should first meet curve I as follows:

$$F_{FI} = F_{xb1} = F_{hy\_F} + F_{reg1} \tag{8}$$

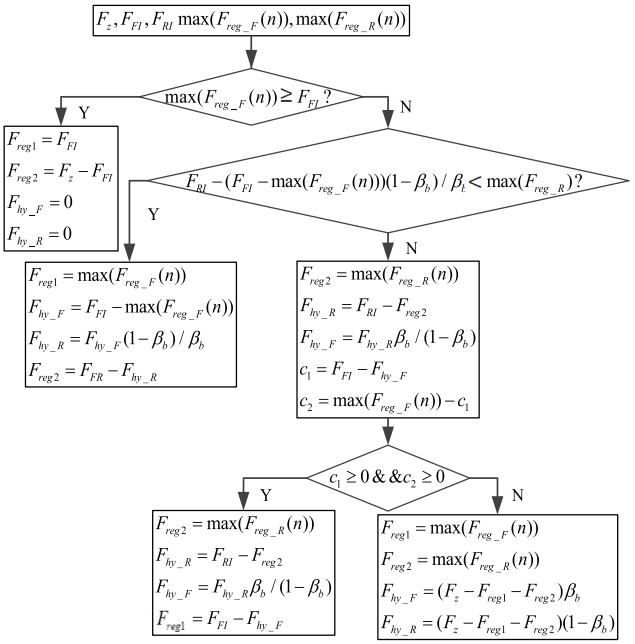

FIGURE 4. Control algorithm logic of braking force distribution between front axle and rear axle.

The maximum braking force of electric motor is the function of motor speed n. So the maximum braking force of front motor and rear motor are written as $max\left(F_{reg\_F}(n)\right)$ and $max\left(F_{reg\_R}(n)\right)$, respectively. The control algorithm logic of braking force distribution is proposed as shown in Figure 4.

(1) If $max\left(F_{reg\_F}(n)\right) \geq F_{FI}$, $max\left(F_{reg\_F}(n)\right)$ can meet F_{FI}. So the electric motor braking force and hydraulic braking force of front axle are defined as:

$$F_{reg1} = F_{FI} \tag{9}$$
$$F_{hy\_F} = 0 \tag{10}$$

For the 4WD EV in this study, the braking force required by rear wheel is smaller than that of front wheel in braking ($F_{FI} > F_{RI}$). Because the front and rear motors of the FWD EV are the same, $max\left(F_{reg\_R}(n)\right)$ can also meet F_{RI}. Thus the electric motor braking force and hydraulic braking force of rear axle are defined as:

$$F_{reg2} = F_{RI} = F_z - F_{FI} \tag{11}$$
$$F_{hy\_R} = 0 \tag{12}$$

(2) If $max\left(F_{reg\_F}(n)\right) < F_{FI}$, the hydraulic braking force of front axle is expressed as:

$$F_{hy\_F} = F_{FI} - max\left(F_{reg\_F}(n)\right) \tag{13}$$

And the hydraulic braking force of front axle can be obtained:

$$F_{hy\_R} = F_{hy\_F}(1-\beta_b)/\beta_b \tag{14}$$

where β_b represents the hydraulic braking force distribution relationship of the front and rear axles, and is given as $\beta_b = F_{hy\_F}/\left(F_{hy\_F} + F_{hy\_R}\right)$.

In this study, the RBS is developed for a low-cost 4WD EV. So it is assumed that the hydraulic braking force distribution relationship of the front and rear wheels is fixed, and β_b is a fixed value. In this case, two situations are considered:

1) If $max\left(F_{reg\_R}(n)\right) + F_{hy\_R} \geq F_{RI}$, the electric motor braking force of rear axle is defined as:

$$F_{reg2} = F_{RI} - F_{hy\_R} \tag{15}$$

2) If $max\left(F_{reg\_R}(n)\right) + F_{hy\_R} < F_{RI}$, rear wheels are not locked. The electric motor braking force of rear axle is defined as:

$$F_{reg2} = max\left(F_{reg\_R}(n)\right) \tag{16}$$

According to curve I, the hydraulic braking force of rear axle can be increased as:

$$F_{hy\_R} = F_{RI} - max\left(F_{reg\_R}(n)\right) \tag{17}$$

And the hydraulic braking force of front axle is updated as:

$$F_{hy\_F} = F_{hy\_R}\beta_b/(1-\beta_b) \tag{18}$$

In this case, another two situations are considered as follows:

(a) If $F_{FI} \geq F_{hy\_F}$ & $max\left(F_{reg\_F}(n)\right) + F_{hy\_F} \geq F_{FI}$, the electric motor braking force of front axle is defined as:

$$F_{reg1} = F_{FI} - F_{hy\_F} \tag{19}$$

(b) Otherwise, the electric motor braking force and hydraulic braking force of the front and rear axles are defined as:

$$\begin{cases} F_{reg1} = max\left(F_{reg\_F}(n)\right) \\ F_{reg2} = max\left(F_{reg\_R}(n)\right) \\ F_{hy\_F} = \left(F_z - F_{reg1} - F_{reg2}\right)\beta_b \\ F_{hy\_R} = \left(F_z - F_{reg1} - F_{reg2}\right)(1-\beta_b) \end{cases} \tag{20}$$

According to the braking force distribution strategy above, the controller model of braking energy recovery strategy based on curve I is established in Matlab/Simulink as shown in Figure 5.

IV. SIMULATIONS AND RESULTS ANALYSIS

The proposed braking energy recovery strategy in Section 3 is validated using the vehicle system model built in Section 2 through the numerical simulations under different fixed braking strength and continuously varying braking strength, respectively. We assume that the road pavement is straight and homogeneous with a uniform tire-road adhesion coefficient of 0.85. The initial SOC of battery is set to 40%. The vehicle is first accelerated to a speed of 80 km/h at full load, and then is decelerated by braking at different braking strength.

During braking, the total braking energy can be obtained by the following equation:

$$E_k = \frac{1}{2}mv_0^2 \tag{21}$$

where E_k is the total braking energy. m is the mass of vehicle and load. v_0 is the initial braking speed.

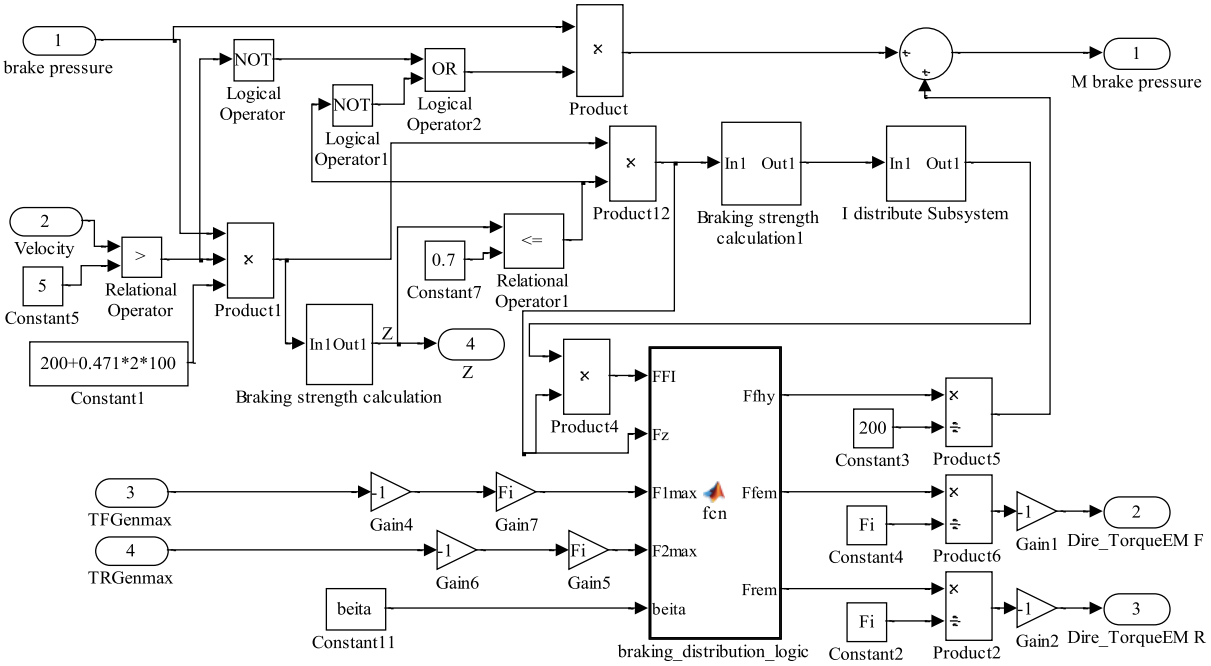

FIGURE 5. Controller model of braking energy recovery strategy in Matlab/Simulink.

The recovery rate of braking energy can be expressed as:

$$\eta = \frac{E_b}{E_k} \times 100\% \tag{22}$$

where E_b is the energy recovered by the RBS.

A. SIMULATIONS OF DIFFERENT FIXED BRAKING STRENGTH

The braking simulations are carried out under three braking strength, which are low braking strength ($z = 0.10$), medium braking strength ($z = 0.35$), and emergency braking strength ($z = 0.75$).

The simulation results under low braking strength ($z = 0.10$) are shown in Figure 6. Figure 6 (a) shows the driving and braking torque responses of the front and rear wheels from motors and hydraulic braking. Because the simulation is carried out on straight and homogeneous road, it only shows the driving-braking torque responses of left wheels. Figure 6 (b) shows the battery energy responses in charge and discharge. From the figures, it can be seen the vehicle is in acceleration phase from 0 s to 19.56 s and then starts to brake. In acceleration phase, the driving torque responses of the front and rear wheels are the same, which present a driving torque output with constant torque characteristics at low speed and with constant power characteristics at high speed. The regenerative braking function starts to work at 19.56 s, and turn off at 37.65 s with the hydraulic braking system starting work at the same time. Obviously, the motor braking force of the front and rear axles can fully meet the vehicle's braking requirement under low braking strength ($z = 0.10$).

The simulation results under medium braking strength ($z = 0.35$) are shown in Figure 7. From Figure 7 (a), it can be seen that the motor braking force of the front and rear

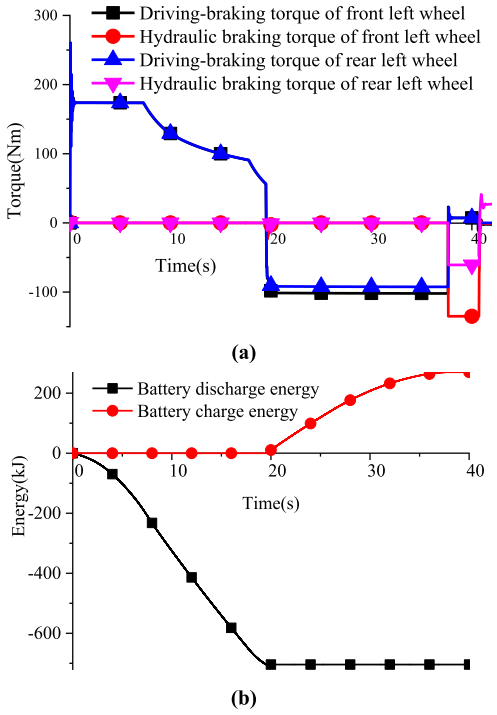

FIGURE 6. Simulation results under low braking strength ($z = 0.10$). (a) Driving-braking torque responses of the front and rear wheels. (b) Battery energy responses in charge and discharge.

axles can not meet the vehicle's braking requirement under medium braking strength ($z = 0.35$), so the hydraulic braking system is working together at the same time. For this reason, the braking energy recovered under medium braking strength ($z = 0.35$) is less than that in low braking strength ($z = 0.10$). In addition, it can be found that the regenerative braking force of the front motor reaches the maximum value of its external characteristics, but that of the rear motor does not

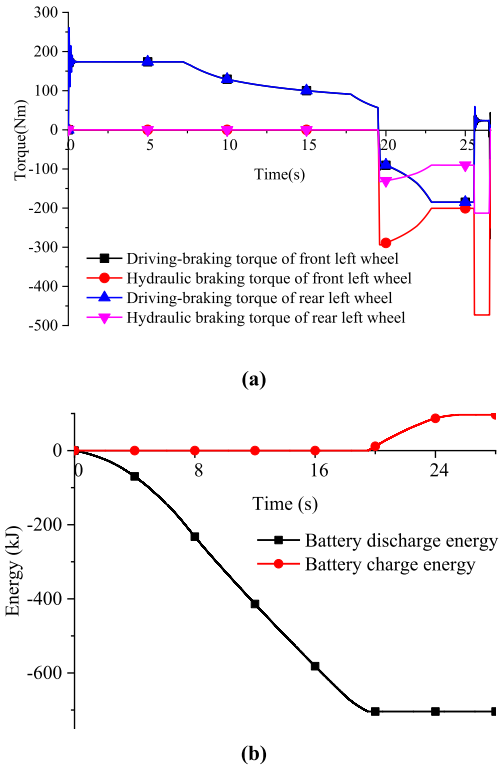

FIGURE 7. Simulation results under medium braking strength. ($z = 0.35$). (a) Driving-braking torque responses of the front and rear wheels. (b) Battery energy responses in charge and discharge.

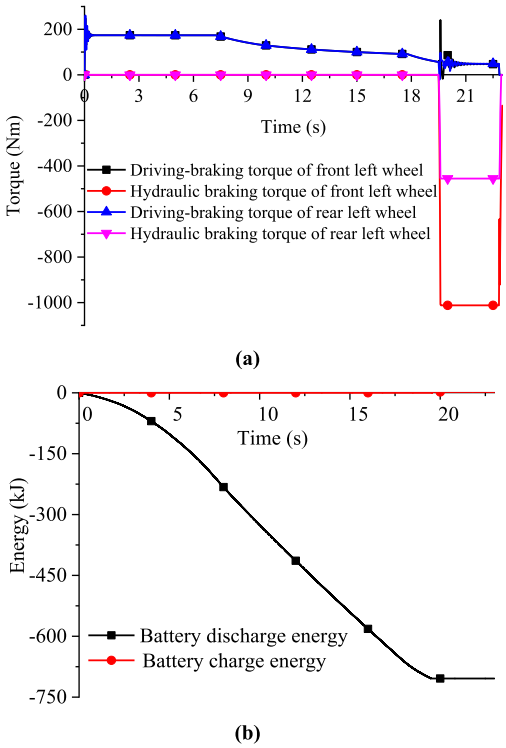

FIGURE 8. Simulation results under emergency braking strength ($z = 0.75$). (a) Driving-braking torque responses of the front and rear wheels. (b) Battery energy responses in charge and discharge.

reach the maximum value. It's mainly due to the control strategy of braking energy recovery in this study. In order to ensure braking stability, the braking force of front axle is designed to meet curve I first. Because the motor braking force of front axle can not meet the braking requirement of curve I, the hydraulic braking force of front wheel increases to make up for it, which leads to the increase of the hydraulic braking force of rear wheel according to the fixed distribution relationship β_b. So the regenerative braking force of the rear motor does not reach the maximum value.

Obviously, the control strategy in this study can not achieve the maximum capacity of braking energy recovery for the vehicle with fixed hydraulic braking force distribution of the front and rear wheels under medium strength braking. If the hydraulic braking force distribution of the front and rear wheels can be adjusted freely, the braking energy can be recovered to maximum, but it will increase the cost of the vehicle braking system.

The simulation results under emergency braking strength ($z = 0.75$) are shown in Figure 8. Obviously, the front and rear motors do not participate in braking, the hydraulic braking force of the front and rear wheels are distributed according to β_b. In this case, there is no braking energy being recovered and charging the battery.

According to (21) and (22), the total braking energy, recovered braking energy, and braking energy recovery rate under different braking strength can be obtained, which is listed in Table 4. In view of braking energy recovery rate,

TABLE 4. Comparison of brake energy recovery under different braking strength.

Braking strength z	Total braking energy E_k (kJ)	Recovered energy E_b (kJ)	Energy recovery rate η (%)
0.10	343.49	269.88	78.55
0.35	343.49	96.45	28.80
0.75	343.49	0	0

the vehicle achieves the highest braking energy recovery rate of 78.55% under low braking strength ($z = 0.10$). In case of medium braking strength ($z = 0.35$), the braking energy recovery rate is not very high owing to the consumption of hydraulic braking. In emergency braking, the motor's regenerative braking function is turned off, and there is no braking energy being recovered.

B. SIMULATIONS OF CONTINUOUSLY VARING BRAKING STRENGTH

The simulation is carried out under a continuously varying braking strength as shown in Figure 9. The vehicle is in acceleration phase from 0 s to 19.56 s and then starts to brake. Figure 10 shows the driving-braking torque responses of the front and rear wheels. It can be seen that regenerative braking of the front and rear motors start to work at 19.56 s, and turn off at 28.50 s. The motor braking force responses of the front and rear axles are the same. When they can not meet the braking requirement of curve I, the hydraulic braking system starts to work together with them. Figure 11 shows the

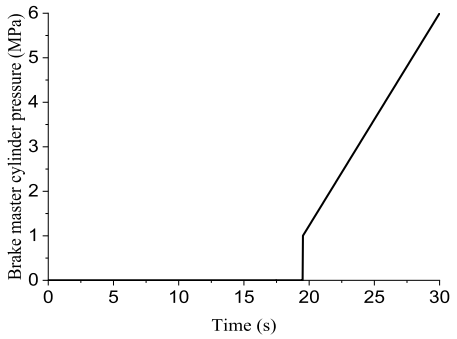

FIGURE 9. Brake master cylinder pressure corresponding to continuously varying braking strength.

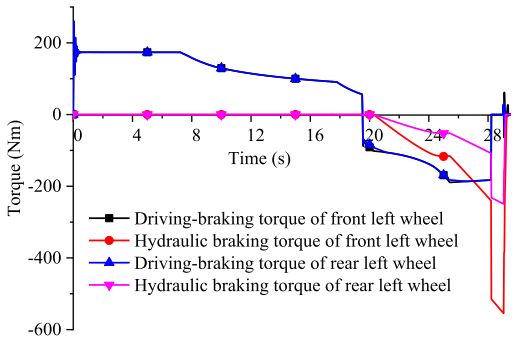

FIGURE 10. Driving-braking torque responses of the front and rear wheels.

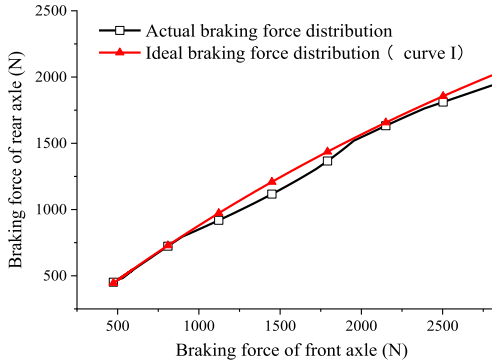

FIGURE 11. Comparison of actual braking force distribution with curve I.

comparison of actual braking force distribution with curve I. It can be found the actual braking force distribution of the front and rear axles can meet the braking requirement of curve I in low braking strength. As the braking strength increases, it begins to deviate downward from curve I to ensure braking stability.

The simulation results above show that the proposed braking energy recovery strategy is able to achieve the regenerative braking function under both different fixed braking strength and continuously varying braking strength while ensuring the braking efficiency and braking stability.

V. CONCLUSION

Aiming at the characteristic that the braking energy recovery of small EVs is mainly concentrated in the stage of low and medium braking strength, an improved braking energy recovery strategy based on ideal braking force distribution (curve I) was proposed for the RBS of a small FWD EV. Compared with previous study, the improved braking energy recovery strategy gives more consideration to braking stability and covers broader and more realistic braking situations of the vehicle.

And then, the braking energy recovery strategy is extensively validated through numerical simulations of a previously built vehicle system model under different fixed braking strength and continuously varying braking strength. In model simulations, it can achieve the braking energy recovery rate of about 79% under low braking strength and about 29% under medium braking strength. The simulation results show that the proposed braking energy recovery strategy is able to effectively achieve the regenerative braking function under different braking conditions while ensuring the braking efficiency and braking stability.

REFERENCES

[1] H.-Z. Wang, G.-Q. Li, G.-B. Wang, J.-C. Peng, H. Jiang, and Y.-T. Liu, "Deep learning based ensemble approach for probabilistic wind power forecasting," *Appl. Energy*, vol. 188, pp. 56–70, Feb. 2017.

[2] H. Wang, Z. Lei, X. Zhang, B. Zhou, and J. Peng, "A review of deep learning for renewable energy forecasting," *Energy Convers. Manage.*, vol. 198, Oct. 2019, Art. no. 111799.

[3] H. Wang, Y. Liu, B. Zhou, C. Li, G. Cao, N. Voropai, and E. Barakhtenko, "Taxonomy research of artificial intelligence for deterministic solar power forecasting," *Energy Convers. Manage.*, vol. 214, Jun. 2020, Art. no. 112909.

[4] H. Z. Wang, G. B. Wang, G. Q. Li, J. C. Peng, and Y. T. Liu, "Deep belief network based deterministic and probabilistic wind speed forecasting approach," *Appl. Energy*, vol. 182, pp. 80–93, Nov. 2016.

[5] Y. Zhu, H. Wu, and J. Zhang, "Regenerative braking control strategy for electric vehicles based on optimization of switched reluctance generator drive system," *IEEE Access*, vol. 8, pp. 76671–76682, 2020.

[6] W. Xu, H. Chen, J. Wang, and H. Zhao, "Velocity optimization for braking energy management of in-wheel motor electric vehicles," *IEEE Access*, vol. 7, pp. 66410–66422, 2019.

[7] Q. Xu, F. Wang, X. Zhang, and S. Cui, "Research on the efficiency optimization control of the regenerative braking system of hybrid electrical vehicle based on electrical variable transmission," *IEEE Access*, vol. 7, pp. 116823–116834, 2019.

[8] D. Paul, E. Velenis, D. Cao, and T. Dobo, "Optimal μ-estimation-based regenerative braking strategy for an AWD HEV," *IEEE Trans. Transp. Electrific.*, vol. 3, no. 1, pp. 249–258, Mar. 2017.

[9] V. V. S. N. Murty and A. Kumar, "Multi-objective energy management in microgrids with hybrid energy sources and battery energy storage systems," *Protection Control Mod. Power Syst.*, vol. 5, no. 1, pp. 1–20, Dec. 2020.

[10] G. Yan, D. Liu, J. Li, and G. Mu, "A cost accounting method of the li-ion battery energy storage system for frequency regulation considering the effect of life degradation," *Protection Control Mod. Power Syst.*, vol. 3, no. 1, pp. 43–51, Dec. 2018.

[11] X. Zhang, D. Gohlich, and J. Li, "Energy-efficient toque allocation design of traction and regenerative braking for distributed drive electric vehicles," *IEEE Trans. Veh. Technol.*, vol. 67, no. 1, pp. 285–295, Jan. 2018.

[12] D. Xu, Q. Wu, B. Zhou, C. Li, L. Bai, and S. Huang, "Distributed multi-energy operation of coupled electricity, heating and natural gas networks," *IEEE Trans. Sustain. Energy*, early access, Dec. 23, 2020, doi: 10.1109/TSTE.2019.2961432.

[13] W. Li, H. Du, and W. Li, "Four-wheel electric braking system configuration with new braking torque distribution strategy for improving energy recovery efficiency," *IEEE Trans. Intell. Transp. Syst.*, vol. 21, no. 1, pp. 87–103, Jan. 2020.

[14] G. Xu, K. Xu, C. Zheng, X. Zhang, and T. Zahid, "Fully electrified regenerative braking control for deep energy recovery and maintaining safety of electric vehicles," *IEEE Trans. Veh. Technol.*, vol. 65, no. 3, pp. 1186–1198, Mar. 2016.
[15] X. Yuan, L. Li, H. Gou, and T. Dong, "Energy and environmental impact of battery electric vehicle range in China," *Appl. Energy*, vol. 157, pp. 75–84, Nov. 2015.
[16] H. Yeo and H. Kim, "Hardware-in-the-loop simulation of regenerative braking for a hybrid electric vehicle," *Proc. Inst. Mech. Eng., D, J. Automobile Eng.*, vol. 216, no. 11, pp. 855–864, Nov. 2002.
[17] H. Yeo, S. Hwang, and H. Kim, "Regenerative braking algorithm for a hybrid electric vehicle with CVT ratio control," *Proc. Inst. Mech. Eng., D, J. Automobile Eng.*, vol. 220, no. 11, pp. 1589–1600, Nov. 2006.
[18] H. Shu, D. Qin, M. Hu, Y. L. Yang, and M. Ye, "Regenerative braking energy management strategy for mild hybrid electric vehicles," (in Chinese), *J. Mech. Eng.*, vol. 45, no. 1, pp. 167–173, Jan. 2009.
[19] J. W. Ko, S. Y. Ko, I. S. Kim, D. Y. Hyun, and H. S. Kim, "Co-operative control for regenerative braking and friction braking to increase energy recovery without wheel lock," *Int. J. Automot. Technol.*, vol. 15, no. 2, pp. 253–262, Mar. 2014.
[20] J. Ko, S. Ko, H. Son, B. Yoo, J. Cheon, and H. Kim, "Development of brake system and regenerative braking cooperative control algorithm for Automatic-Transmission-Based hybrid electric vehicles," *IEEE Trans. Veh. Technol.*, vol. 64, no. 2, pp. 431–440, Feb. 2015.
[21] G. Arnold, "Simulation of advanced regenerative braking strategies in a series plug-in hybrid electric vehicle," International Powertrains, Fuels & Lubricants Meeting, SAE Int. 2017-2466, 2017.
[22] B. Li, H. Du, and W. Li, "A potential field approach-based trajectory control for autonomous electric vehicles with in-wheel motors," *IEEE Trans. Intell. Transp. Syst.*, vol. 18, no. 8, pp. 2044–2055, Aug. 2017.
[23] K. Itani, A. De Bernardinis, Z. Khatir, and A. Jammal, "Comparison between two braking control methods integrating energy recovery for a two-wheel front driven electric vehicle," *Energy Convers. Manage.*, vol. 122, pp. 330–343, Aug. 2016.
[24] J. Ruan, P. D. Walker, P. A. Watterson, and N. Zhang, "The dynamic performance and economic benefit of a blended braking system in a multi-speed battery electric vehicle," *Appl. Energy*, vol. 183, pp. 1240–1258, Dec. 2016.
[25] D. Sun, F. Lan, and J. Chen, "A study on the braking energy recovery strategy for a 4WD battery electric vehicle based on ideal braking force distribution (curve I)," (in Chinese), *Automot. Eng.*, vol. 35, no. 2, pp. 1057–1061, 2013.
[26] F. Wang, H. Zhong, Z. Ma, X. Mao, and B. Zhuo, "Regenerative braking of hybrid power system in coasting mode," (in Chinese), *J. South China Univ. Technol. (Natural Sci.)*, vol. 37, no. 7, pp. 62–68, 2009.
[27] F. Wang, X. Yin, H. Luo, and Y. Huang, "A series regenerative braking control strategy based on hybrid-power," in *Proc. Int. Conf. Comput. Distrib. Control Intell. Environ. Monitor.*, Mar. 2012, pp. 65–69.
[28] C. Chen and M. Lin, "Adaptive-learning regeneration controller design for electric vehicles," in *Proc. SAE World Congr. Exhib.*, Detroit, MI, USA, Apr. 2013.
[29] D. Sun, F. Lan, Y. Zhou, and J. Chen, "Control algorithm of electric vehicle in coasting mode based on driving feeling," *Chin. J. Mech. Eng.*, vol. 28, no. 3, pp. 479–486, May 2015.
[30] F. Ji, Y. Pan, Y. Zhou, F. Du, Q. Zhang, and G. Li, "Energy recovery based on pedal situation for regenerative braking system of electric vehicle," *Vehicle Syst. Dyn.*, vol. 58, no. 1, pp. 144–173, Jan. 2020.
[31] D. Sun, F. Lan, X. He, and J. Chen, "Study on adaptive acceleration slip regulation for dual-motor four-wheel drive electric vehicle," (in Chinese), *Automot. Eng.*, vol. 38, no. 5, pp. 600–608, May 2016.
[32] D. Sun, F. Lan, X. He, and J. Chen, "Self-adaptive composite ABS of dual-motor four-wheel drive electric vehicle," (in Chinese), *J. Jilin Univ. (Eng. Technol. Ed.)*, vol. 46, no. 5, pp. 1405–1413, Sep. 2016.

ZHENGWEI MA received the B.E. degree in transportation from the North China University of Water Resources and Electric Power, China, in 2010, and the Ph.D. degree in vehicle engineering from the South China University of Technology, China, in 2015. He has been an Assistant Professor with the College of Mechatronics and Control Engineering, Shenzhen University, since 2015. He has been an Assistant Professor and then an Associate Professor with the College of Urban Transportation and Logistics, Shenzhen Technology University, since 2017. His research interests include the design, control, and optimization in energy efficiency, safety, man-machine of smart, and sustainable mobility, especially for electric vehicles.

DAXU SUN received the M.E. degree in mechanical design and theory from Henan Polytechnic University, in 2006, and the Ph.D. degree in vehicle engineering from the South China University of Technology, China, in 2015. He has been an Associate Professor with the School of Automobile Engineering, Foshan Polytechnic, since 2020. His research interests include the design, control, and optimization in control systems of the electric vehicle and the self-driving car.